Editors' Suggestion

Fourth- and Fifth-Order Virial Coefficients from Weak Coupling to Unitarity

Y. Hou and J. E. Drut
Department of Physics and Astronomy, University of North Carolina, Chapel Hill, North Carolina 27599, USA

(Received 27 April 2020; accepted 8 July 2020; published 28 July 2020)

In the current era of precision quantum many-body physics, one of the most scrutinized systems is the unitary limit of the nonrelativistic spin-1/2 Fermi gas, due to its simplicity and relevance for atomic, condensed matter, and nuclear physics. The thermodynamics of this strongly correlated system is determined by universal functions which, at high temperatures, are governed by universal virial coefficients b_n that capture the effects of the n-body system on the many-body dynamics. Currently, b_2 and b_3 are well understood, but the situation is less clear for b_4, and no predictions have been made for b_5. To answer these open questions, we implement a nonperturbative analytic approach based on the Trotter-Suzuki factorization of the imaginary-time evolution operator, using progressively finer temporal lattice spacings. By means of these factorizations and automated algebra codes, we obtain the interaction-induced change Δb_n from weak coupling to unitarity. At unitarity, we find that $\Delta b_3 = -0.356(4)$ in agreement with previous results, $\Delta b_4 = 0.062(2)$, which is in agreement with all previous theoretical estimates but at odds with experimental determinations, and $\Delta b_5 = 0.078(6)$, which is a prediction. We show the impact of those answers on the density equation of state and Tan contact, and trace their origin back to their polarized and unpolarized components.

DOI: 10.1103/PhysRevLett.125.050403

Introduction.—With the advances in precise ultracold atom experiments on one hand, and new and powerful algorithms and machines on the other, quantum many-body physics has in many ways entered a precision era. Experimentally, ultracold atoms are arguably the cleanest and most malleable systems [1], and also those where an ever-increasing number of observables can be measured with unprecedented precision [2]. On the computational side, progress has been steady in a wide range of areas: from advanced benchmarks of paradigmatic condensed matter systems like the Hubbard model [3] to percent-level calculations in lattice QCD [4].

In this broad quantum many-body context, one of the most sought-after systems, due to its relevance to atomic, condensed matter, and nuclear physics, is the unitary limit of the three-dimensional spin-1/2 Fermi gas [5]. This system is remarkable for its deceptive simplicity: it is just a two-species Fermi gas with an attractive zero-range interaction, tuned to the threshold of two-body bound-state formation (i.e., infinite scattering length). While simple to define, the problem is challenging for many-body theory, as there are no small parameters to perform a controlled expansion. In nature, the system is realized approximately in dilute neutron matter in the crust of neutron stars [6] and practically exactly in ultracold-atom experiments [2]. In the latter, Feshbach resonances enable varying the coupling strength by dialing an external magnetic field [7], such that a large portion of the so-called BCS-BEC crossover (which contains the unitary limit) can be realized and explored [8–10]. The strongly coupled region around unitarity is also interesting due to its strong pairing correlations, which modify both the superfluid phase as well as the normal phase [11,12]. Crucially, the unitary limit features a nonrelativistic conformal invariance [13], which is responsible for its hallmark property of *universality* [14]: it is characterized by dimensionless functions that are insensitive to the details of the underlying interactions.

Experiments realizing the unitary Fermi gas can achieve temperatures low enough to probe the superfluid state, but also high enough to access the normal state and the quantum-classical crossover. The latter is also of relevance to nuclear astrophysics [15–17] and is characterized by the virial expansion [18], whose behavior is determined by *universal* virial coefficients b_n (universal in the sense of being independent from temperature as well as from the microscopic details of the interaction). At nth order, these coefficients capture the thermodynamic contributions of the n-body system. While the calculation of b_n of noninteracting gases is a textbook example, the interacting counterpart poses a challenging problem, especially so as n is increased beyond $n = 2$. Below, we will use the noninteracting value $b_n^{(0)} = (-1)^{n+1} n^{-5/2}$ as a reference and work in terms of the interaction-induced change $\Delta b_n = b_n - b_n^{(0)}$. The second-order case is given by the celebrated Beth-Uhlenbeck (BU) formula [19,20]

$$\Delta b_2 = \frac{e^{\lambda^2}}{\sqrt{2}}[1 + \mathrm{erf}(\lambda)], \tag{1}$$

where $\lambda = \sqrt{\beta}/a_0$, a_0 is the s-wave scattering length, and β is the inverse temperature. (The unitary limit corresponds to $\lambda = 0$; in this Letter we will focus on the $\lambda \leq 0$ sector.) Meanwhile, the third-order coefficient Δb_3 is much more challenging to compute and has been approached numerically [21] as well as analytically [22–26], at and away from unitarity. In turn, work on Δb_4 has largely focused on the unitary limit [27–30] (see however Ref. [31]). Notably, while there is good agreement on Δb_3 between theory and experiment [32,33], the situation is less clear for Δb_4, as we explain below. There have been no estimates of Δb_5, to the best of our knowledge.

In this Letter, we contribute to the exploration of the quantum-classical crossover by calculating Δb_4 and Δb_5 (along with their counterparts for polarized systems) for spin-1/2 fermions with attractive interactions, covering from weak coupling to the unitary limit. To that end, we implement and progressively refine a factorization of the Boltzmann weight, extrapolating to the continuum limit of that factorization at the end. Our method is similar to the one originally advocated in Ref. [34] but with dramatic improvements and optimizations that enabled the present work. Below, we outline the formalism and basic aspects of the method, leaving the most technical details for the Supplemental Material [35].

Hamiltonian, virial expansion, and computational method.—The Hamiltonian that describes dilute, two-species Fermi gases is $\hat{H} = \hat{T} + \hat{V}$, where

$$\hat{T} = \sum_{s=\uparrow,\downarrow} \int d^3x \hat{\psi}_s^\dagger(\mathbf{x}) \left(-\frac{\hbar^2 \nabla^2}{2m} \right) \hat{\psi}_s(\mathbf{x}), \tag{2}$$

and

$$\hat{V} = -g \int d^3x \hat{n}_\uparrow(\mathbf{x}) \hat{n}_\downarrow(\mathbf{x}), \tag{3}$$

where $\hat{\psi}_s, \hat{\psi}_s^\dagger$ are the fermionic field operators for particles of spin $s = \uparrow, \downarrow$, and $\hat{n}_s(\mathbf{x}) = \hat{\psi}_s^\dagger(\mathbf{x})\hat{\psi}_s(\mathbf{x})$ are the coordinate-space densities. In the remainder of this Letter, we will take $\hbar = k_B = m = 1$. The contact interaction is singular in three-dimensional space, such that regularization and renormalization are needed (see below).

The virial expansion is an expansion of the equilibrium many-body problem around the dilute limit $z \to 0$, where $z = e^{\beta\mu}$ is the fugacity and μ the chemical potential coupled to the total particle number operator $\hat{N}$. In powers of z, the grand-canonical partition function is

$$\mathcal{Z} = \mathrm{tr}[e^{-\beta(\hat{H}-\mu\hat{N})}] = \sum_{N=0}^{\infty} z^N Q_N, \tag{4}$$

where $Q_N = \mathrm{tr}_N[\exp(-\beta\hat{H})]$ is the N-body partition function. Calling $\mathcal{Z}_0$ the noninteracting limit of $\mathcal{Z}$, we may write the virial expansion for the pressure P (relative to the noninteracting pressure P_0) as

$$\beta(P - P_0)V = \ln(\mathcal{Z}/\mathcal{Z}_0) = Q_1 \sum_{n=2}^{\infty} \Delta b_n z^n, \tag{5}$$

where V is the system volume, $Q_1 = 2V/\lambda_T^3$ is the single-particle partition function, $\lambda_T = \sqrt{2\pi\beta}$ is the thermal wavelength, and the interaction-induced change Δb_n is related to the interaction change ΔQ_N by Taylor-expanding the logarithm of Eq. (4) (and its noninteracting counterpart) around $z = 0$ (see, e.g., Ref. [34] for explicit formulas). To evaluate the ΔQ_N relevant for Δb_n, we introduce a Trotter-Suzuki (TS) factorization of the imaginary-time evolution operator

$$e^{-\beta\hat{H}} \simeq (e^{-\beta\hat{T}/(2k)} e^{-\beta\hat{V}/k} e^{-\beta\hat{T}/(2k)})^k, \tag{6}$$

which defines the kth order in the proposed approximation. When calculating Q_N, Eq. (6) will appear inside a trace, such that the remainder scales as $\sim k^{-2}$. Our code calculates symbolically the diagonal matrix elements of the right-hand side of Eq. (6) in a complete set of Slater determinant multiparticle states (built out of plane-wave single-particle states), inserting completeness relations between kinetic- and potential-energy factors as needed. The resulting momentum sums become Gaussian integrals in the continuum limit (see below), which are carried out analytically and automatically. Previous work carried out calculations at $k = 1$ for Δb_n up to $n = 4$ (the so-called semiclassical approximation of Refs. [34,45,46]); and $k = 2$ up to $n = 7$ [34]. (See also Ref. [47] for an application of the same technique to systems with three-body forces.) For the calculations presented here, we dramatically improved our implementation, extending our analysis of $n = 3$, 4, 5 for k as large as possible with the computational resources available to us, respectively, $k = 21$, 12, 9.

Renormalization.—To renormalize the contact interaction, we implemented two different procedures, both of them regularized by placing the system on a spatial lattice of spacing ℓ, which is implicitly taken to zero at the end of the calculation by replacing momentum sums with integrals from $-\infty$ to ∞. These renormalization procedures, which yield consistent results at large-enough order k in Eq. (6) (see also [35]), are as follows.

The first way is to tune the lattice theory so that the order-k factorized calculation of Δb_2 matches the continuum value set by the BU formula Eq. (1) (e.g., $\Delta b_2 = 1/\sqrt{2}$ at unitarity). To that end, we tune the dimensionless coupling $\tilde{C}$ [35] to reproduce the desired dimensionless value of Δb_2. This is the same renormalization procedure used in Refs. [34,45,46] and it amounts to following the "line of constant Δb_2" as k is varied.

The second way to renormalize is more conventional: at a given factorization order k, we tune the coupling so as to reproduce the largest eigenvalue of the exact two-body transfer matrix, namely $\exp(-\beta E_0/k)$, where E_0 is the exact two-body ground-state energy. The matrix elements of the order-k factorized transfer matrix can be easily computed, in particular in the center-of-mass frame. Using those matrix elements, it is easy to see [35] that the desired $\tilde{C}$ is given by

$$\tilde{C} = \frac{1}{(2\pi x)^{\frac{3}{2}}} \lim_{\Lambda\to\infty} \left[\sum_{\mathbf{a}}^{\Lambda} \frac{1}{\exp[-\frac{4\pi^2 x}{k}(\eta_0^2 - \mathbf{a}^2)] - 1} \right]^{-1}, \quad (7)$$

where $x = \beta/L^2$, L is the size of system, and $\mathbf{a}$ is a three-component integer vector. Here, η_0^2 is set by the ground-state energy and given by Lüscher's formula [48]; at unitarity $\eta_0^2 \simeq -0.0959$. Taking the continuum limit amounts to opening the length scale window $\ell \ll \lambda_T \ll L$, which corresponds to calculating $\tilde{C}$ in the limit $\Lambda \to \infty$ and $x \to 0$. This procedure follows the "line of constant E_0" as k is varied. Since Δb_2 is sensitive to the whole energy spectrum, not just the ground-state energy E_0, the two procedures yield answers which differ at finite k, but which must be consistent at large enough k if the continuum limit is approached. We show our consistency checks in [35].

Results.—Using the methods described above, we obtained estimates for Δb_n, for $n = 3, 4, 5$ by extrapolating to the large-k limit, with uncertainties in our answers resulting from that extrapolation [35]. The results are shown in Fig. 1, where we parametrize the coupling strength using the ratio $\Delta b_2/\Delta b_2^{\mathrm{UFG}}$, where $\Delta b_2^{\mathrm{UFG}} = 1/\sqrt{2}$ is the value of Δb_2 at unitarity. [The corresponding scattering length can be obtained via Eq. (1).]

As mentioned above, Δb_3 was estimated numerically as well as (semi)analytically by several authors [21,23–26], and is by now a well-understood number; at unitarity it is $\Delta b_3^{\mathrm{UFG}} \simeq -0.3551$ (we quote only the first few digits of the exact-diagonalization result of Ref. [21], which is enough for our needs here). We obtain $\Delta b_3^{\mathrm{UFG}} = -0.356(4)$ which, while not as precise as previous determinations, agrees with them. Our results are also in excellent agreement with Leyronas' analytic result [24].

Also shown in Fig. 1 (top) are our results for Δb_4, compared with prior theoretical estimates of its value at unitarity $\Delta b_4^{\mathrm{UFG}}$. Our result $\Delta b_4^{\mathrm{UFG}} = 0.062(2)$ at face value compares well with every other theoretical estimate (see however our subspace discussion below), namely Yan and Blume [29]: $\Delta b_4^{\mathrm{UFG}} = 0.078(18)$; Endo and Castin [30]: $\Delta b_4^{\mathrm{UFG}} = 0.0620(8)$, and Ngampruetikorn *et al.* [31]: $\Delta b_4^{\mathrm{UFG}} = 0.06$. While the last two are a conjecture and an approximate result, respectively, Yan and Blume's is a Monte Carlo result with a comparatively large uncertainty encompassing all prior theoretical estimates. Our calculation, like Yan and Blume's, comes from a first-principles nonperturbative approach but does not incur statistical errors and thus provides a substantial reduction in the overall uncertainty.

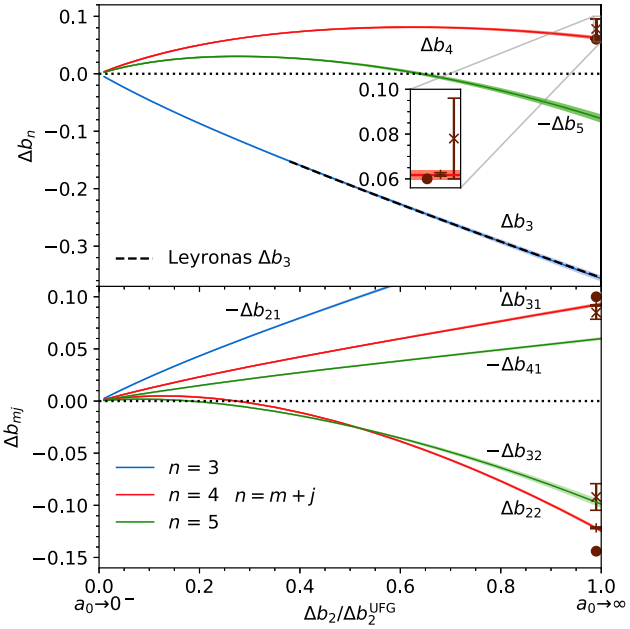

FIG. 1. Top: our results for Δb_3 (blue), Δb_4 (red), and $-\Delta b_5$ (green) shown with error bands as functions of the coupling strength given by $\Delta b_2/\Delta b_2^{\mathrm{UFG}}$. (We plot $-\Delta b_5$ to avoid display interference with Δb_4 around unitarity.) The dashed line shows Δb_3 from Ref. [24]. The dark red cross (with errorbar) shows the Monte Carlo results of Ref. [29]: $\Delta b_4^{\mathrm{UFG}} = 0.078(18)$; the dark red plus sign (with small error bar) indicates the conjecture of Ref. [30]: $\Delta b_4^{\mathrm{UFG}} = 0.0620(8)$; finally, the dark red dot shows the approximate results of Ref. [31]: $\Delta b_4^{\mathrm{UFG}} = 0.06$. Bottom: subspace contributions Δb_{mj} as functions of the coupling strength. Our results are shown as error bands, color coded as in the top plot by $n = m + j$: blue for Δb_{21}, red for Δb_{31} and Δb_{22}, and green for Δb_{41} and Δb_{32}. The red cross (with errorbar) shows Ref. [29]: $\Delta b_{31}^{\mathrm{UFG}} = 0.0848(64)$ and $\Delta b_{22}^{\mathrm{UFG}} = -0.0920(128)$; the red dot shows Ref. [31]: $\Delta b_{31}^{\mathrm{UFG}} = 0.100$ and $\Delta b_{22}^{\mathrm{UFG}} = -0.144$; finally, the red plus sign (with small error bar) shows Ref. [30]: $\Delta b_{31}^{\mathrm{UFG}} = 0.09188(16)$ and $\Delta b_{22}^{\mathrm{UFG}} = -0.1220(8)$. Our results are closest to the latter; we obtain $\Delta b_{31}^{\mathrm{UFG}} = 0.0931(8)$ and $\Delta b_{22}^{\mathrm{UFG}} = -0.1244(7)$.

There have also been attempts to determine $\Delta b_4^{\mathrm{UFG}}$ from experimental data on the equation of state [e.g., ENS [32]: 0.096(15), and MIT [33]: 0.096(10); see also our Fig. 2 (top)]. However, those analyses face a challenging numerical problem, namely fitting a fourth-order polynomial with no knowledge of the size of higher order contributions or where the fourth order truly dominates; we return to this below. While the Monte Carlo result of Ref. [29] overlaps with the above analyses, our result disagrees with them (as do Refs. [30,31]). [However, it may be argued that a 2σ error analysis of the ENS's and our results brings them into marginal agreement.]

To understand the origin of our $\Delta b_4^{\mathrm{UFG}}$, we refer to Fig. 1 (bottom), which shows the two components that

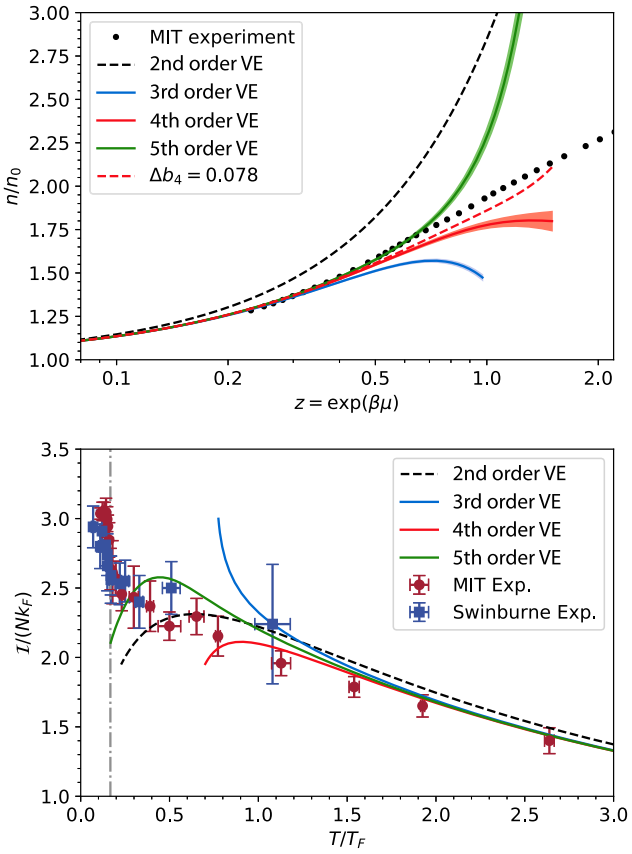

FIG. 2. Top: density equation of state at unitarity as a function of the fugacity z showing our virial expansion results (error bands) compared with the data of Ref. [33]. The fourth-order virial expansion is also shown using the central value for Δb_4 of Ref. [29]. Bottom: tan contact at unitarity as a function of temperature T in units of the Fermi temperature $T_F = (3\pi^2 n)^{2/3}/2$, where n is the density, compared with the experimental measurements of Refs. [49,50]. The vertical dash-dotted line shows the critical temperature $T_c/T_F = 0.167(13)$ of Ref. [33].

make up the full result $\Delta b_4 = 2\Delta b_{31} + \Delta b_{22}$: the polarized sector Δb_{31} and the unpolarized sector Δb_{22} (defined in [35]). For essentially all couplings studied here, Δb_{31} is increasingly positive and Δb_{22} increasingly negative as unitarity is approached, which results in the nonmonotonic behavior of Δb_4 in Fig. 1 (top), and its low value at unitarity. Figure 1 (bottom) also yields a more detailed comparison with prior theoretical approaches at unitarity. Specifically, at the 95% confidence level [51] our result for Δb_{31} overlaps with Endo and Castin [30] but not with Yan and Blume [29] nor with Ngampruetikorn *et al.* [31]. On the other hand, at the same level our Δb_{22} also overlaps with Endo and Castin [30] and marginally with Yan and Blume [29], but not with Ngampruetikorn *et al.* [31]. This analysis suggests that the closer agreement for Δb_4 at unitarity shown in the top panel of Fig. 1 is due at least in part to error compensation between Δb_{31} and Δb_{22}.

For the fifth-order virial coefficient at unitarity we obtain $\Delta b_5^{\mathrm{UFG}} = 0.078(6)$, which is the first estimate of this universal quantity, to the best of our knowledge. Figure 1 (top) shows Δb_5 as a function of the coupling. As with Δb_4, the nonmonotonicity of Δb_5 can be traced back to the competition between two sectors with (largely) monotonic but opposite behavior. As shown in Fig. 1 (bottom), Δb_{41} and Δb_{32} become progressively more negative and more positive, respectively, as the coupling is increased (with the exception of a small region at very weak couplings where Δb_{32} is negative). Thus, $\Delta b_5 = 2\Delta b_{41} + 2\Delta b_{32}$ is nonmonotonic; furthermore, it changes sign from negative to positive around $\Delta b_2/\Delta b_2^{\mathrm{UFG}} \simeq 0.63$ and proceeds to grow in magnitude enough to overtake Δb_4. This is notable because the "normal" ordering $|\Delta b_3| > |\Delta b_4| > |\Delta b_5|$ is preserved from weak couplings up to $\Delta b_2/\Delta b_2^{\mathrm{UFG}} \simeq 0.96$, but $|\Delta b_5| > |\Delta b_4|$ after that, in particular at unitarity. Crucially, such a large Δb_5 could easily interfere with the experimental determination of Δb_4, which would explain the discrepancies between our results and the experimental equation-of-state analyses of Δb_4.

TABLE I. Estimates for Δb_3 to Δb_5 in the unitary limit, including the subspace coefficients for the polarized case Δb_{mj}.

	$n = 3$	$n = 4$	$n = 5$
$\Delta b_n^{\mathrm{UFG}}$	−0.356(4)	0.062(2)	0.078(6)
$\Delta b_{(n-1)1}^{\mathrm{UFG}}$	−0.178(2)	0.0931(8)	−0.0598(7)
$\Delta b_{(n-2)2}^{\mathrm{UFG}}$	…	−0.1244(7)	0.0988(29)

The subspace contributions Δb_{mj} mentioned above allow us to study the first steps of the "polaron sequence" Δb_{m1}. Beyond the qualitative resemblance of $|\Delta b_{m1}|$ for all m, we find that $|\Delta b_{m1}|$ decreases as m is increased for all the couplings we studied (see Table I in particular), which we interpret as due to the largely noninteracting majority particles (as the interaction is of zero range). Furthermore, we observe that the sequence alternates in sign, which we conjecture will persist for arbitrary m.

In a harmonic trapping potential of frequency ω, the b_n (being dimensionless) acquire a dependence on $\beta\omega$. In the high-temperature limit $\beta\omega \to 0$, the relationship $\Delta b_n^T(\beta\omega) \to \Delta b_n^T = \Delta b_n/n^{3/2}$ holds [21], where $\Delta b_n^T(\beta\omega)$ is the trapped coefficient, and Δb_n^T its high-temperature limit. At unitarity, $\Delta b_2^T = 1/4$, and we find $\Delta b_3^T = -0.0685(8)$, $\Delta b_4^T = 0.00775(25)$, and $\Delta b_5^T = 0.0070(5)$. Notably, the factor $n^{-3/2}$ restores the "normal order" $|\Delta b_3^T| > |\Delta b_4^T| > |\Delta b_5^T|$, in contrast to the homogeneous case, supporting the notion that trapping potentials enhance the convergence of the virial expansion [21].

Finally, in Fig. 2 (top) we use our results to obtain the density equation of state and compare with the experiment of Ref. [33]. While our results at fourth order are somewhat farther away from the data than those of Ref. [29], the fifth-order contribution considerably improves the agreement for $z = 0.5$–0.73. In Fig. 2 (bottom) we compare our results

for the Tan contact [52–54] with the measurements of Refs. [49,50]. For clarity, we only compare with experiments; we include theoretical approaches and the polarized case in [35]. Our fifth-order results appear to follow the trend of the experimental data for temperatures as low as $T/T_F \simeq 0.45$.

Summary and conclusions.—In this work we have performed a fully nonperturbative calculation of the fourth- and fifth-order virial coefficients of attractively interacting spin-1/2 fermions, from weak coupling to the unitary limit. To that end, we implemented a TS factorization of the imaginary-time evolution operator, using progressively finer temporal lattice spacings and extrapolating to the continuous-time limit. The traces of these factorizations were calculated analytically using automated algebra to access the canonical partition functions that yield the interaction-induced changes Δb_n. We found that the universal values at unitarity are $\Delta b_3^{\mathrm{UFG}} = -0.356(4)$, in agreement with previous calculations; $\Delta b_4^{\mathrm{UFG}} = 0.062(2)$, in agreement with previous theoretical estimates (see however our subspace discussion around Fig. 1) but at odds with experimental equation-of-state analyses; and finally $\Delta b_5^{\mathrm{UFG}} = 0.078(6)$, which is a prediction. We also presented the subspace contributions Δb_{31}, Δb_{22}, Δb_{41}, and Δb_{32}, which tend to grow in magnitude with the coupling strength but come with opposite sign and thus compete within Δb_n. The Δb_{ij} are important as they govern the virial expansion of polarized gases (see, e.g., [55]). To show the impact of our $\Delta b_4^{\mathrm{UFG}}$ and $\Delta b_5^{\mathrm{UFG}}$, we compared with the experimental determination of the density equation of state and the Tan contact. Our answers yield an improvement over lower orders, which is remarkable considering the size of the contributions and that the system is strongly correlated.

We would like to thank J. Braun, A. Bulgac, H. Hu, L. Rammelmüller, A. Richie-Halford, C. Vale, and M. W. Zwierlein for comments on the manuscript. We are also grateful to the authors of Refs. [24,49,50] for kindly providing us with their data. This material is based upon work supported by the National Science Foundation under Grant No. PHY1452635.

[1] M. Lewenstein, A. Sanpera, and V. Ahufinger, *Ultracold Atoms in Optical Lattices: Simulating Quantum Many-Body Systems* (Oxford University Press, New York, 2012).

[2] *Ultracold Fermi Gases, Proceedings of the International School of Physics "Enrico Fermi", Course CLXIV, Varenna, 2006*, edited by M. Inguscio, W. Ketterle, and C. Salomon (IOS Press, Amsterdam, 2008).

[3] J. P. F. LeBlanc *et al.*, Solutions of the Two-Dimensional Hubbard Model: Benchmarks and Results from a Wide Range of Numerical Algorithms, Phys. Rev. X **5**, 041041 (2015).

[4] C. C. Chang, A. N. Nicholson, E. Rinaldi, E. Berkowitz, and N. Garron, A per-cent-level determination of the nucleon axial coupling from quantum chromodynamics, Nature (London) **558**, 91 (2018).

[5] *The BCS-BEC Crossover and the Unitary Fermi Gas*, edited by W. Zwerger (Springer-Verlag, Berlin, 2012).

[6] C. J. Pethick and D. G. Ravenhall, Matter at large neutron excess and the physics of neutron-star crusts, Annu. Rev. Nucl. Part. Sci. **45**, 429 (1995).

[7] C. Chin, R. Grimm, P. Julienne, and E. Tiesinga, Feshbach resonances in ultracold gases, Rev. Mod. Phys. **82**, 1225 (2010).

[8] I. Bloch, J. Dalibard, and W. Zwerger, Many-body physics with ultracold gases, Rev. Mod. Phys. **80**, 885 (2008).

[9] S. Giorgini, L. P. Pitaevskii, and S. Stringari, Theory of ultracold Fermi gases, Rev. Mod. Phys. **80**, 1215 (2008).

[10] G. C. Strinati, P. Pieri, G. Röpke, P. Schuck, and M. Urban, The BCS-BEC crossover: From ultra-cold fermi gases to nuclear systems, Phys. Rep. **738**, 1 (2018).

[11] E. J. Mueller, Review of pseudogaps in strongly interacting fermi gases, Rep. Prog. Phys. **80**, 104401 (2017).

[12] A. Richie-Halford, J. E. Drut, and A. Bulgac, Emergence of a pseudogap in the BCS-BEC crossover, arXiv:2004.05014.

[13] Y. Nishida and D. T. Son, Nonrelativistic conformal field theories, Phys. Rev. D **76**, 086004 (2007).

[14] T. L. Ho, Universal Thermodynamics of Degenerate Quantum Gases in the Unitarity Limit, Phys. Rev. Lett. **92**, 090402 (2004).

[15] C. J. Horowitz and A. Schwenk, The virial equation of state of low-density neutron matter, Phys. Lett. B **638**, 153 (2006).

[16] C. J. Horowitz and A. Schwenk, The neutrino response of low-density neutron matter from the virial expansion, Phys. Lett. B **642**, 326 (2006).

[17] C. J. Horowitz and A. Schwenk, Cluster formation and the virial equation of state of low-density nuclear matter, Nucl. Phys. **A776**, 55 (2006).

[18] X.-J. Liu, Virial expansion for a strongly correlated Fermi system and its application to ultracold atomic Fermi gases, Phys. Rep. **524**, 37 (2013).

[19] E. Beth and G. E. Uhlenbeck, The quantum theory of the non-ideal gas. II. Behaviour at low temperatures, Physica (Utrecht) **4**, 915 (1937).

[20] D. Lee and T. Schäfer, Cold dilute neutron matter on the lattice. I. Lattice virial coefficients and large scattering lengths, Phys. Rev. C **73**, 015201 (2006).

[21] X.-J. Liu, H. Hu, and P. D. Drummond, Virial expansion for a strongly correlated Fermi gas, Phys. Rev. Lett. **102**, 160401 (2009).

[22] P. F. Bedaque and G. Rupak, Dilute resonating gases and the third virial coefficient, Phys. Rev. B **67**, 174513 (2003).

[23] D. B. Kaplan and S. Sun, A New Field Theoretic Method for the Virial Expansion, Phys. Rev. Lett. **107**, 030601 (2011).

[24] X. Leyronas, Virial expansion with Feynman diagrams, Phys. Rev. A **84**, 053633 (2011).

[25] Y.Castin and F. Werner, Le troisiéme coefficient du viriel du gaz de Bose unitaire, Can. J. Phys. **91**, 382 (2013).

[26] C. Gao, S. Endo, and Y. Castin, The third virial coefficient of a two-component unitary Fermi gas across an Efimov-effect threshold, Europhys. Lett. **109**, 16003 (2015).

[27] D. Rakshit, K. M. Daily, and D. Blume, Natural and unnatural parity states of small trapped equal-mass two-component Fermi gases at unitarity and fourth-order virial coefficient, Phys. Rev. A **85**, 033634 (2012).
[28] S. Endo and Y. Castin, Absence of a four-body Efimov effect in the $2+2$ fermionic problem, Phys. Rev. A **92**, 053624 (2015).
[29] Y. Yan and D. Blume, Path integral Monte Carlo Determination of the Fourth-Order Virial Coefficient for Unitary Two-Component Fermi Gas with Zero-Range Interactions, Phys. Rev. Lett. **116**, 230401 (2016).
[30] S. Endo and Y. Castin, The interaction-sensitive states of a trapped two-component ideal Fermi gas and application to the virial expansion of the unitary Fermi gas, J. Phys. A **49**, 265301 (2016).
[31] V. Ngampruetikorn, M. M. Parish, and J. Levinsen, High-temperature limit of the resonant Fermi gas, Phys. Rev. A **91**, 013606 (2015).
[32] S. Nascimbene, N. Navon, K. Jiang, F. Chevy, and C. Salomon, Exploring the thermodynamics of a universal Fermi gas, Nature (London) **463**, 1057 (2010).
[33] M. J. H. Ku, A. T. Sommer, L. W. Cheuk, and M. W. Zwierlein, Revealing the superfluid Lambda transition in the Universal thermodynamics of a unitary Fermi gas, Science **335**, 563 (2012).
[34] Y. Hou, A. Czejdo, J. DeChant, C. R. Shill, and J. E. Drut, Leading-order semiclassical approximation to the first seven virial coefficients of spin-1/2 fermions across spatial dimensions, Phys. Rev. A **100**, 063627 (2019).
[35] See the Supplemental Material at http://link.aps.org/supplemental/10.1103/PhysRevLett.125.050403 for technical aspects of the method, extrapolations to the continuous time limit, and results for physical quantities, which includes Refs. [36–44].
[36] O. Goulko and M. Wingate, Numerical study of the unitary Fermi gas across the superfluid transition, Phys. Rev. A **93**, 053604 (2016).
[37] R. Rossi, T. Ohgoe, E. Kozik, N. Prokof'ev, B. Svistunov, K. Van Houcke, and F. Werner, Contact and Momentum Distribution of the Unitary Fermi Gas, Phys. Rev. Lett. **121**, 130406 (2018).
[38] T. Enss, R. Haussmann, and W. Zwerger, Viscosity and scale invariance in the unitary Fermi gas, Ann. Phys. (Amsterdam) **326**, 770 (2011).
[39] F. Palestini, A. Perali, P. Pieri, and G. C. Strinati, Temperature and coupling dependence of the universal contact intensity for an ultracold Fermi gas, Phys. Rev. A **82**, 021605 (2010).
[40] H. Hu, X.-J. Liu, and P. D. Drummond, Universal contact of strongly interacting fermions at finite temperatures, New J. Phys. **13**, 035007 (2011).
[41] Z. Yan, P. B. Patel, B. Mukherjee, R. J. Fletcher, J. Struck, and M. W. Zwierlein, Boiling a Unitary Fermi Liquid, Phys. Rev. Lett. **122**, 093401 (2019).
[42] M. Pindor, Pade approximants and Borel summation for QCD perturbation expansions, arXiv:hep-th/9903151.
[43] Y. Nishida and D. T. Son, ϵ expansion for a Fermi Gas at Infinite Scattering Length, Phys. Rev. Lett. **97**, 050403 (2006).
[44] P. Arnold, J. E. Drut, and D. T. Son, Next-to-next-to-leading-order ϵ expansion for a Fermi gas at infinite scattering length, Phys. Rev. A **75**, 043605 (2007).
[45] C. R. Shill and J. E. Drut, Virial coefficients of 1D and 2D Fermi gases by stochastic methods and a semiclassical lattice approximation, Phys. Rev. A **98**, 053615 (2018).
[46] K. J. Morrell, C. E. Berger, and J. E. Drut, Third- and fourth-order virial coefficients of harmonically trapped fermions in a semiclassical approximation, Phys. Rev. A **100**, 063626 (2019).
[47] A. J. Czejdo, J. E. Drut, Y. Hou, J. R. McKenney, and K. J. Morrell, Virial coefficients of trapped and un-trapped three-component fermions with three-body forces in arbitrary spatial dimensions, Phys. Rev. A **101**, 063630 (2020).
[48] M. Lüscher, Volume dependence of the energy spectrum in massive quantum field theories, Commun. Math. Phys. **105**, 153 (1986).
[49] C. Carcy, S. Hoinka, M. G. Lingham, P. Dyke, C. C. N. Kuhn, H. Hu, and C. J. Vale, Contact and Sum Rules in a Near-Uniform Fermi Gas at Unitarity, Phys. Rev. Lett. **122**, 203401 (2019).
[50] B. Mukherjee, P. B. Patel, Z. Yan, R. J. Fletcher, J. Struck, and M. W. Zwierlein, Spectral Response and Contact of the Unitary Fermi Gas, Phys. Rev. Lett. **122**, 203402 (2019).
[51] By this we mean doubling the size of the error bars of all the results discussed, with the caveat that it is strictly speaking unknown whether the errors are normally distributed.
[52] S. Tan, Energetics of a strongly correlated Fermi gas, Ann. Phys. (Amsterdam) **323**, 2952 (2008).
[53] S. Tan, Large momentum part of fermions with large scattering length, Ann. Phys. (Amsterdam) **323**, 2971 (2008).
[54] S. Tan, Generalized Virial theorem and pressure relation for a strongly correlated Fermi gas, Ann. Phys. (Amsterdam) **323**, 2987 (2008).
[55] L. Rammelmüller, A. C. Loheac, J. E. Drut, and J. Braun, Finite-Temperature Equation of State of Polarized Fermions at Unitarity, Phys. Rev. Lett. **121**, 173001 (2018).